RESISTANCE CURVES IN THE TENSILE AND COMPRESSIVE LONGITUDINAL FAILURE OF COMPOSITES

Pedro P. Camanho[1], Giuseppe Catalanotti[1] ,Carlos G. Dávila[2], Claudio S. Lopes[1], Miguel A. Bessa[1], José C. Xavier[3]

[1]DEMec, Faculdade de Engenharia, Universidade do Porto,
Rua Dr. Roberto Frias, 4200-465 Porto, Portugal-
E-mail: pcamanho@fe.up.pt

[2]NASA Langley Research Center, Hampton VA, USA

[3]Universidade de Trás-os-Montes e Alto Douro, Portugal

ABSTRACT

This paper presents a new methodology to measure the crack resistance curves associated with fiber-dominated failure modes in polymer-matrix composites. These crack resistance curves not only characterize the fracture toughness of the material, but are also the basis for the identification of the parameters of the softening laws used in the analytical and numerical simulation of fracture in composite materials. The method proposed is based on the identification of the crack tip location by the use of Digital Image Correlation and the calculation of the J-integral directly from the test data using a simple expression derived for cross-ply composite laminates. It is shown that the results obtained using the proposed methodology yield crack resistance curves similar to those obtained using FEM-based methods in compact tension carbon-epoxy specimens. However, it is also shown that the Digital Image Correlation based technique can be used to extract crack resistance curves in compact compression tests for which FEM-based techniques are inadequate.

KEY WORDS: Intralaminar fracture toughness; R-curve; composite laminates; digital image correlation.

1. INTRODUCTION

Despite the significant advances in the analysis models for the prediction of fracture in composite materials, such as advanced failure criteria and associated damage models, sophisticated kinematic representations of fracture mechanisms, and cohesive elements to deal with delamination, the accurate prediction of intralaminar fracture mechanisms, acting at the ply level, still presents several challenges.

The majority of existing models to predict intralaminar fracture of polymer-based composite materials reinforced by carbon fibers are based on softening constitutive models [1]. The shape of the softening law, e.g., linear, exponential or other, is generally assumed to be inconsequential for the prediction of fracture. While this assumption is valid under small-scale bridging conditions, the shape of the cohesive law plays a fundamental role in the prediction of fracture under large-scale bridging conditions, where the process zone length may be large relative to other length scales in the problem [2]. When crack propagation includes different energy dissipation mechanisms that act over different length scales, the nature of these mechanisms must be accounted for in the cohesive law.

Several failure mechanisms including fiber tensile fracture, fiber-matrix pull-out and matrix cracking are present when a crack propagates in a plane perpendicular to the fiber direction. To account for these different failure mechanisms, the authors have proposed in a previous paper a combined linear-exponential softening law for fiber tensile fracture [3], and demonstrated that a simple linear softening law is unable to predict the load-displacement relation obtained in a cross-ply Compact Tension (CT) test specimen, while a bi-linear softening law provides an accurate prediction [4].

For longitudinal compression, the definition of the parameters used in the softening law related to the fiber kinking failure mechanisms is based on the experimental determination of the crack resistance curve (R-curve) of the Compact Compression (CC) test specimen [5]. However, the CC test specimen presents several problems that are yet to be resolved: the tractions that are transferred along a kink band render the numerical calculation of the J-integral using the Finite Element Method (FEM) inaccurate [5]. In addition, the experimental determination of the exact location of the tip of a kink band is difficult.

Therefore, the objective of this paper is to address these problems by using an alternative method that is based on the use of the Digital Image Correlation (DIC) technique. An automatic algorithm that post-processes the data obtained from the DIC system is used to detect

the crack tip location and to establish the R-curve from the surface measurements of the displacement field.

2. CONFIGURATION OF THE TEST SPECIMENS

The material used is the carbon-fiber reinforced epoxy IM7-8552 provided by Hexcel composites. Average values of the material properties of IM7-8552, measured in a previous investigation [6], are shown in Tables 1 and 2.

Table 1. Elastic properties of IM7-8552

E_{1T} (GPa)	E_{1C} (GPa)	E_2 (GPa)	G_{12} (GPa)	υ_{12}
171.4	150	9.1	5.3	0.3

where E_1 and E_2 are, respectively, the ply longitudinal and transverse modulus, G_{12} is the ply shear modulus, and υ_{12} is the ply major Poisson ratio.

Table 2. Strengths of IM7-8552 (MPa)

X_T	X_C	Y_T	Y_T	S_L
2326	1200	62	200	92

where X_T and X_C are respectively the ply longitudinal tensile and compressive strength, Y_T and Y_C are, respectively, the ply transverse tensile and compressive strengths, and S_L is the ply shear strength.

The pre-impregnated plies were laid-up in an $[90/0]_{8s}$ configuration and cured according to Hexcel's specifications. The resulting plates were cut using a diamond-coated saw to their nominal overall dimensions. The specimens were finally machined to their final geometry, shown in Figure 1. The holes for the load introduction points were cut using tungsten – carbide drills and by clamping the specimens between to sacrificial carbon-epoxy plates. This procedure prevents the test specimens from delamination at the entrance and exit of the drill.

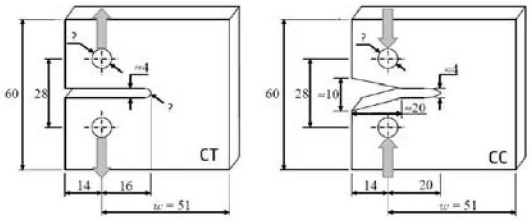

(a) CT specimen (b) CC specimen

Figure 1. Geometry of the CT and CC test specimens (after Pinho [5]).

3. IDENTIFICATION OF THE CRACK TIP LOCATION

The accurate measurement of the crack location is performed by post-processing the information obtained by the DIC system. The function K(P) proposed by Grégoire [7], which identifies a discontinuity inside a pattern based on the observed displacement field. The procedure was modified to enable the identification of crack tips in carbon-epoxy CT and CC test specimens, and implemented in a MATLAB [8] code which provides the following information:

- K(P)=0 - no discontinuity (bulk material).
- K(P)=-1 - discontinuity (crack).
- K(P)=1 - crack tip.

Figure 2 shows the result of the application of the MATLAB algorithm during the crack propagation stage of a CT specimen. The exact location of the crack tip is identified and quantified by the location where K(P)=1. This procedure obviates the need for the visual identification of the crack tip, which is prone to human errors, especially in the case of the CC test specimen.

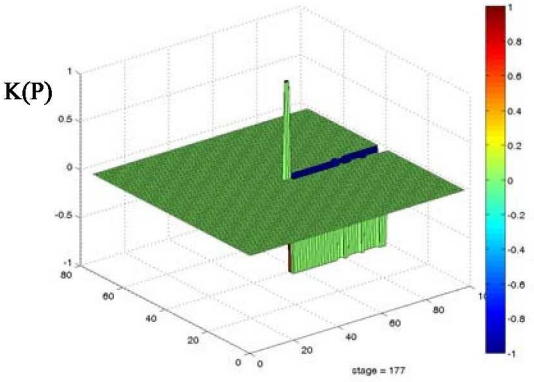

Figure 2. Identification of the crack tip location in a CT test specimen.

4. EXPERIMENTAL DETERMINATION OF THE J-INTEGRAL

A new method to evaluate the J-integral and to measure the crack resistance curve based on the surface displacement and strain fields obtained from a Digital Image Correlation (DIC) system is proposed.

The digital image correlation ARAMIS software developed by GOM [9] was used in this work. This measurement system is equipped with an 8-bit Baumer Optronic FWX20 camera (resolution of 1624x1236 pixels, pixel size of 4.4µm and sensor format of 1/1.8") coupled with a Schneider-Kreuznach Componar-S 50mm f/2.8 lenses. Using DIC, several matrices containing the in-plane displacement and strain fields are obtained; these fields are the basis for the calculation of the J-integral.

For the cross-ply laminate used here, and assuming that there is no bending of the specimen, the J-integral can be defined using classical lamination theory as:

$$J = \frac{t}{2}\int_{\Omega_0}\left(\{\bar{\sigma}\}\{\varepsilon\}^T n_1 - 2\left\{\frac{\partial u}{\partial x_1}\right\}^T [\bar{\sigma}]\{n\}\right) \mathrm{d}s$$

(1)

where the stress tensor, collected in $\{\bar{\sigma}\}$, is averaged through-the-thickness of the laminate and t corresponds to the laminate thickness.

The contour selected to calculate the J-integral from the DIC system is shown in Figure 3.

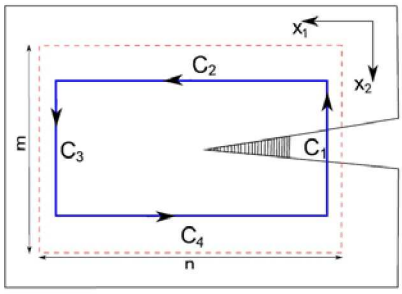

Figure 3. Contour used to calculate the J-integral

4.1. Calculation of the stresses.

The stresses are computed from the homogenized stiffness matrix as: $\{\bar{\sigma}\}=[\bar{C}]\{\varepsilon\}$, where $\{\varepsilon\}$ is the strain matrix calculated at a given position by the DIC.

4.2. Calculation of dx_1, dx_2, and ds.

The differentials dx_1 and dx_2 are taken as the differences between the centers of adjoining macro-pixel windows, measured along the corresponding axes. The differential ds is the Euclidian norm of dx_1 and dx_2.

4.3. Calculation of $\{n\}$

This vector is directly defined by the simple contour sub-divisions shown in Figure 3, taking the following forms: $\{1,0,0\}^T$ on C_3, $\{0,1,0\}^T$ on C_4, $\{-1,0,0\}^T$ on C_1, and $\{0,-1,0\}^T$ on C_2.

4.4. Calculation of $\left\{\frac{\partial u}{\partial x_1}\right\}$

This vector is calculated using the central difference method applied in three adjoining macro-pixels. Having calculated all the terms required in equation (1), the J-integral is computed from the summation of all discrete contributions of each macro-pixel, which are calculated using equation (1) with the relevant terms calculated as explained in the previous points. This methodology was implemented in a MATLAB program that enables the automatic generation of the R-curve by assigning to each crack length the corresponding value of the J-integral.

5. COMPACT TENSION TESTS

The CT test was conducted using an MTS 312.31 testing machine with a load capacity of 250 kN. The tests were performed using a load cell of 100 kN and the speed of the machine used in the displacement controlled test was 2mm/min. Figure 4 shows the set-up used during the CT tests. The test specimen was previously sprayed with a white ink to generate a random distribution of points, as required by the DIC system.

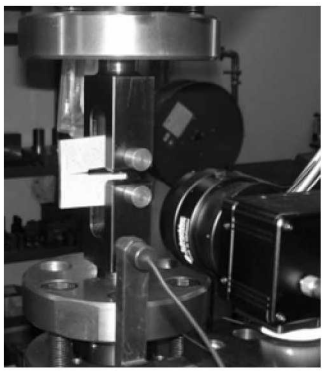

Figure 4. Compact tension test specimen and DIC system.

Figure 5 shows the R-curves measured from the FEM post-processing of the test results obtained by the method proposed by Pinho et al. [4] and those obtained by processing of the displacement and strain fields measured by the DIC system. Figure 5 shows a good correlation between the two techniques.

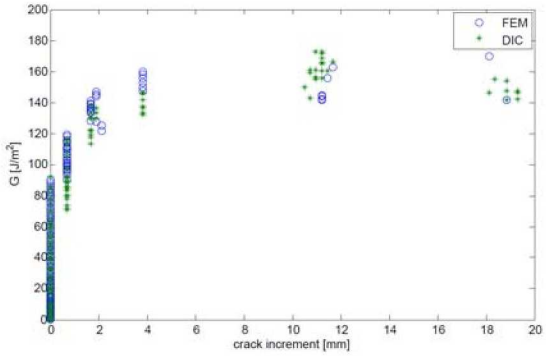

Figure 5. R-curves extracted from a CT specimen using FEM and DIC.

The results show an initial fracture toughness of 92 J/m^2 that steadily increases up to an average toughness of 146 J/m^2 for a crack increment of 4mm. This R-curve results from fiber bridging, as shown in Figure 6.

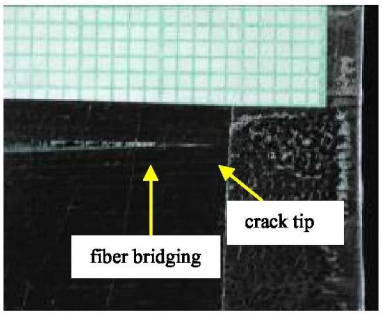

Figure 6. CT test specimen showing fiber bridging.

6. COMPACT COMPRESSION TESTS

The CC tests were conducted with the same test machine and speed as those used in the CT tests. As previously explained, the FEM-based calculation of the J-integral is not appropriate to the calculation of the R-curve because it does not account for the contact and load transfer across the kink band. Figure 7 shows that the FEM-based and DIC-based R-curves differ approximately by a factor of two. At large crack increments (>11 mm.), the FEM-based solution yields unrealistically high values of the fracture toughness that could result in an unreliable softening law for the fiber kinking failure mode.

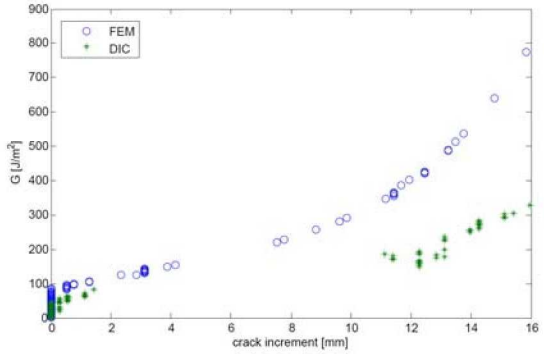

Figure 7. R-curves extracted from a CC specimen using FEM and DIC.

The initiation values of the fracture toughness are also different: approximately 80 J/m^2 for the DIC-based solution and 100 J/m^2 for the FEM-based solution. In addition, the algorithm developed to detect the exact location of the tip of the kink band was unable to yield reliable results for kink band lengths between 2mm and 11mm. The reason for this uncertainty is the presence of a delamination associated with the propagation of the kink band, which pollutes the data in the vicinity of the tip of the kink band.

Figure 8 shows the propagation of the kink band from the initial notch and illustrates the difficulty in detecting the exact location of the tip of the kink band by visual inspection alone. Figure 8 also shows the delamination that accompanies the propagation of the kink band.

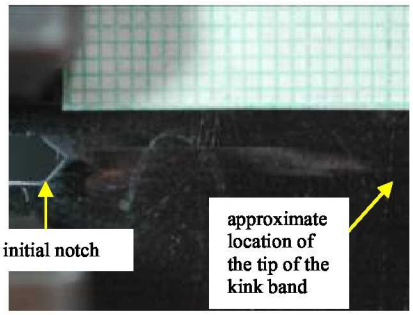

Figure 8. CT test specimen showing the propagation of a kink band.

7. CONCLUSIONS

The displacement and strain fields obtained using DIC during the CT and CC tests of composite laminates may serve as the basis for the rigorous determination of the location of the crack or kink band tips and for the automatic computation of the J-integral. The models develop for these purposes were implemented in a MATLAB code that obviates the need of any complex pre-and post-processing, either based on FEM or standard data reduction methods. In addition, the proposed methodology can be used to generate R-curves for CC tests. Some difficulties encountered in the identification of the tip of the kink-band in the presence of delamination still need to be addressed.

The carbon-epoxy material system used, IM7-8552, shows an R-curve for fiber dominated failure modes under tensile loads, where the fracture toughness increases from 92 J/m^2 to 146 J/m^2. An even more pronounced R-curve was obtained for fiber dominated failure modes under compressive loads, where the fracture toughness ranges from 80 J/m^2 to approximately 300 J/m^2 for large kink band lengths.

ACKNOWLEDGEMENTS

The second author acknowledges the financial support of the European Commission under Contract No. MRTN-CT-2005-019198.

REFERENCES

[1] Lapczyk, I. and Hurtado, J.A., "Progressive damage modeling in fiber-reinforced materials," *Composites Part A*, 38, pp. 2333-2341, 2007.

[2] Sørensen, B.F. and Jacobsen T.K. (1998) "Large-scale bridging in composites: R-curves and bridging laws," *Composites Part A*, 29, pp. 1443-1451, 1998.

[3] Maimí P., Camanho P.P., Mayugo J.A., and Dávila C.G., A continuum damage model for composite laminates: Part I - Constitutive model. *Mechanics of Materials*, 39, pp. 897-908, 2007.

[4] Dávila, C.G., Rose, C.A., and Camanho, P.P., "R-curve toughening in the longitudinal fracture of composites and associated cohesive law," *International Journal of Fracture*, 158, pp. 211-223, 2009.

[5] Pinho, S.T., Robinson P., and Iannucci L., "Fracture toughness of the tensile and compressive fibre failure modes in laminated composites," *Composites Science and Technology*, 66, pp. 2069-2079, 2006.

[6] Camanho, P.P., Maimí, P., and Dávila, C.G., "Prediction of size effects in notched laminates using continuum damage mechanics," *Composites Science and Technology*, 67, pp. 2715-2727, 2007.

[7] Grégoire, D., *Initiation, propagation, arrêt et redémarrage de fissures sous impact*, PhD Thesis, LaMCoS - INSA de Lyon, 2008.

[8] MATLAB, Software Package, Ver. 7.0, The MathWorks, Inc., Natick, MA, 2004.

[9] GOM Optical Measuring Techniques, ARAMIS 3D Deformation Measurement, www.gom.com, Widen, Switzerland, 2009.